

EFFECT OF ENSO-INDUCED CLIMATE VARIABILITY ON GROUNDWATER LEVELS IN THE LOWER APALACHICOLA-CHATTAHOCHEE-FLINT RIVER BASIN

S. Mitra, P. Srivastava, S. Singh, D. Yates

ABSTRACT. *Rapid population growth, urban sprawl, and increased agricultural production in the Apalachicola-Chattahoochee-Flint (ACF) river basin are threatening the availability of freshwater resources and greatly affecting the supply of freshwater to Apalachicola Bay, which supports a struggling shellfish industry. As a result, Alabama, Georgia, and Florida have been fighting over the allocation of ACF river basin water for the past three decades. The water conflict heats up every time there is drought in the basin. In the Southeast U.S., droughts are mainly caused by the La Niña phase of the seasonal-to-interannual climate variability phenomenon known as the El Niño Southern Oscillation (ENSO). Understanding and quantifying the impact of ENSO-induced climate variability on precipitation, soil moisture, streamflows, and groundwater levels can provide valuable information for sustainable management of water resources in this region. This study was undertaken to quantify the impact of ENSO on groundwater levels in the lower ACF river basin, an area highly dependent on groundwater for agricultural water use. Twenty-one observation wells with 30 years of monthly groundwater level data were used to study the ENSO-groundwater level relationship. Wavelet analysis techniques were used to study the teleconnection between ENSO and groundwater levels, while Mann-Whitney tests were conducted to quantify the impact. The effect of prolonged La Niña events on groundwater levels and their corresponding recovery periods were also studied. Results indicate a strong relationship between groundwater level fluctuations and ENSO. This relationship was found to be stronger during the recharge season (December-April) as compared to the non-recharge or agricultural irrigation season (May-November). The results obtained can be used to develop procedures for forecasting groundwater levels, which can then be used to better manage the groundwater resources of this region.*

Keywords. *Droughts, El Niño Southern Oscillation, ENSO, Groundwater, Irrigation, Wavelet analysis.*

Natural climate variability phenomena such as the El Niño Southern Oscillation (ENSO), North Atlantic Oscillation (NAO), and Pacific Decadal Oscillation (PDO) affect precipitation, temperature, and streamflows and can significantly alter the behavior of extreme events such as hurricanes, floods, droughts, and cold waves (IPCC, 2001). Among these phenomena, ENSO-induced climate variability is one of the major causes of natural variability in the global climate system (Diaz and Markgraf, 1992). Identification, understanding, and quantification of this variability are important for minimizing the effects of ENSO on water resources and agriculture (NRC, 1995).

ENSO is a complex ocean-atmospheric phenomenon that occurs in the equatorial Pacific Ocean and has three

phases: El Niño, La Niña, and neutral (oceanic component). El Niño and La Niña refer to the warm and cool phases, respectively, of sea surface temperatures (SST) in the central Pacific Ocean that lead to changes in climatic conditions around the world (Quinn, 1974; Aceituno, 1992). Several indices, including Niño-1+2, Niño-3, Niño-4, and Niño-3.4, have been derived based on SST anomalies. ENSO has been found to affect temperature and precipitation around the world (Chiew et al., 1998; Roy, 2006; Keener et al., 2007). ENSO has also been shown to affect groundwater, streamflow, monsoon, droughts, flood frequency, and crop yield in different parts of the world (McCabe and Dettinger, 1999; Kahya and Dracup, 1993; Gurdak et al., 2007; Chiew et al., 1998; Rajagopalan and Lall, 1998; Kulkarni, 2000; Roy, 2006; Keener et al., 2007; Tootle et al., 2005; Hansen et al., 2001).

In the Southeast U.S., rapid population growth, urban sprawl, and increased agricultural production in the Apalachicola-Chattahoochee-Flint (ACF) river basin are threatening the availability of freshwater resources and greatly affecting the supply of freshwater to Apalachicola Bay, which supports a struggling shellfish industry. This stress on the basin's water resources is further exacerbated by the large seasonal-to-interannual climate variability experienced by this region. Climate variability in the Southeast is mainly influenced by ENSO, which the primary reason for

Submitted for review in April 2014 as manuscript number SW 10748; approved for publication by the Soil & Water Division of ASABE in August 2014. Presented at the 2013 ASABE Annual Meeting as Paper No. 1045708.

The authors are **Subhasis Mitra, ASABE Member**, Graduate Student, **Puneet Srivastava, ASABE Member**, Professor, and **Sarmistha Singh**, Graduate Student, Department of Biosystems Engineering, Auburn University, Auburn, Alabama; **David Yates**, Scientist, Research Application Laboratory, National Center for Atmospheric Research, Boulder, Colorado. **Corresponding author:** Subhasis Mitra, Tom E. Corley Building, Auburn University, Auburn, AL 36849; phone: 334-332-8165; e-mail: szm0048@auburn.edu.

droughts in the Southeast (Enfield et al., 2001). The El Niño phase of ENSO is characterized by cooler and wetter (than normal) winters, while the La Niña phase is characterized by warmer and drier winters in the Southeast U.S. (Kiladis and Diaz, 1989; Hansen and Maul, 1991a, 1991b; Schmidt and Luther, 2002).

ENSO has been found to affect rainfall, water quality, and streamflow in the watersheds of Alabama, Georgia, and Florida (Sharda et al., 2012; Schmidt et al., 2001; Keener et al., 2010; Johnson et al., 2013). ENSO-induced droughts during 2000-2001, 2007, and 2010-2012 caused losses in agricultural productivity, prompted water-use restrictions, and intensified long-term conflicts among competing water interests in neighboring states, i.e., the “tri-state water wars” between Alabama, Georgia, and Florida (SELC, 2014). Over the last two decades, this conflict has been marked by litigation and failed negotiations. One of the major aspects of the conflict is the streamflow reduction in the Flint River (FR) during droughts due to increased pumping for irrigation, municipal, and industrial purposes from surface and groundwater sources in southwest Georgia.

Agriculture in southwest Georgia is heavily dependent on irrigation water withdrawals from surface and groundwater sources. In this region, groundwater sites outnumber surface water sites, and groundwater withdrawal can run into hundreds of millions of gallons per day. During La Niña events, excessive irrigation from the Upper Floridan Aquifer (UFA), which is the major groundwater-bearing unit, can cause lowering of groundwater levels in the aquifer and reduce streamflows due to the hydrologic connection between the UFA and FR. Additionally, unhindered exploitation of the groundwater resources in the UFA may not be sustainable in the long term. Large groundwater withdrawals adversely affect groundwater levels, particularly during dry periods and in areas where the aquifer is overlaid by thick overburden conditions that severely limit aquifer recharge (Torak and Painter, 2006; Jones and Torak, 2006). This reduction in groundwater levels due to irrigation can cause further reduction in streamflow levels at places where the stream and aquifer are hydrologically connected. Irrigation-induced streamflow reduction in the FR also contributes to water quality degradation, high-temperature issues, and endangered/threatened species concerns in the Apalachicola River, downstream of the FR (fig. 1).

Georgia’s major drought management policy, The Flint River Drought Protection Act (formulated to compensate farmers for not irrigating their crops in the event of drought to avoid irrigation-induced streamflow reduction), has failed in solving the water conflicts in the region, owing to the ineffectiveness of the policy and lack of funds. Due to the complexity of water management issues, the failure of present drought management policies, and the importance of groundwater resources for agricultural, municipal, and industrial purposes in the watershed, it is important to understand the relationships between ENSO-induced droughts and groundwater levels in the region. This study is part of a larger project that aims at understanding the relationships between droughts, irrigation, and groundwater levels, with

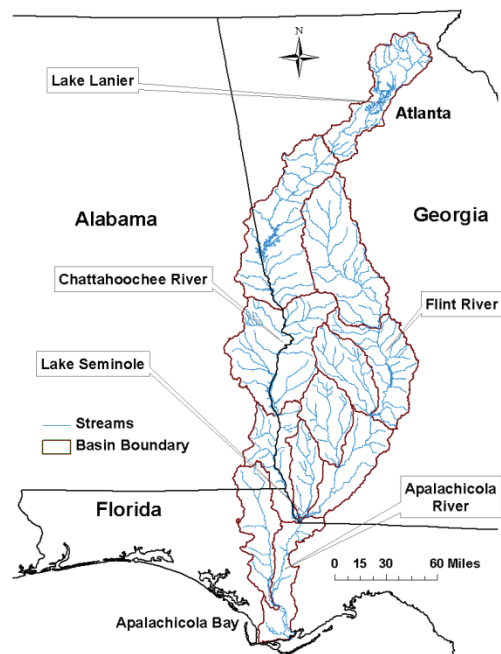


Figure 1. Apalachicola-Chattahoochee-Flint (ACF) river basin. Most of the basin lies in Georgia, the Chattahoochee River forms the boundary between Alabama and Georgia, and the Chattahoochee and Flint Rivers meet in Lake Seminole at the Georgia-Florida border to form the Apalachicola River.

the ultimate goal of developing a methodology for forecasting (seasonal) groundwater levels. The groundwater level forecasting methodology will help stakeholders (farmers and state agencies) avoid irrigation-induced streamflow reductions during drought periods and will help state agencies formulate alternate drought management policies and resolve the complex water management issues and conflicts in the region. In this study, the link between ENSO-induced climate variability and groundwater levels in the lower ACF river basin was explored using wavelet analysis. Non-parametric Mann-Whitney tests were used to quantify the impact. Effects of severe droughts on groundwater levels and recovery periods were also studied to present a complete picture of ENSO-induced droughts on groundwater levels in the region.

MATERIALS AND METHOD

STUDY AREA

The study area is located in the lower ACF river basin in parts of southwestern Georgia, northwestern Florida, and southeastern Alabama (fig. 2). The climate of the lower ACF river basin is humid subtropical, with long summers and mild winters. The average annual temperature and precipitation in the study area are about 18°C (64°F) and 1270 mm (50 in.), respectively. About 4,632 mi² of the land area recharges groundwater that is contained in the karst UFA, which eventually contributes to surface water in the ACF river basin. The UFA system is the major water-bearing formation of the region and consists of aquifers and semi-confining layers with four distinct hydrogeologic units: the surficial aquifer system, the upper semi-confining

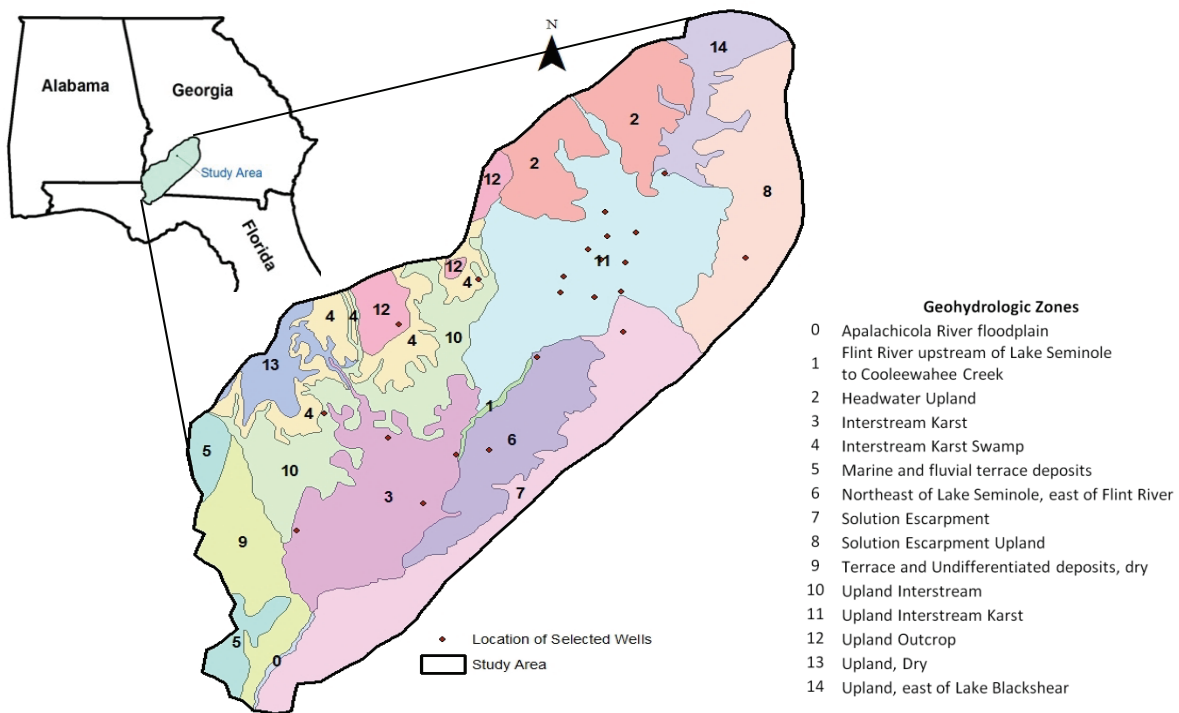


Figure 2. Location of the study area, observation wells, and geohydrologic zones (modified from Torak and Painter, 2006).

unit (USCU), the UFA, and the lower confining unit (Torak and Painter, 2006). These hydrogeologic units are defined by differences in hydraulic characteristics and lithology, which might not coincide with the geologic unit boundaries. The USCU, lying above the UFA, is the major source of vertical leakage to the UFA.

Groundwater levels in the UFA respond to seasonal climatic effects, such as changes in precipitation, temperature, and stream and lake stage, in addition to stresses such as groundwater withdrawal for agricultural, municipal, and industrial purposes. Fluctuations in groundwater levels in the UFA also depend on aquifer thickness and location in the ACF river basin, hydraulic characteristics of the USCU, proximity to surface streams or lake system, and pumping.

ENSO INDEX AND GROUNDWATER DATA

The Niño-3.4 index provided by the National Oceanic and Atmospheric Administration (NOAA) Climate Prediction Center was used for the definition of the ENSO phase (NOAA, 2010). This index is based on 3-month running means of SST anomalies (ERSST.v3b) in the Niño-3.4 region (5° N to 5° S, 120° W to 170° W). The El Niño phase is defined when the Niño-3.4 index is above +0.5°C, while the La Niña phase is defined when the Niño-3.4 index is below -0.5°C. A neutral phase is defined when the Niño-3.4 index is between -0.5°C and +0.5°C. For this study, the middle month of the 3-month running average value of the Niño-3.4 index was assigned to that month.

Daily groundwater (GW) level data for 21 observation wells in the study area were obtained from the U.S. Geological Survey. All the wells were in the UFA, and the pe-

riod of recorded data varied from 25 to 30 years. Time series of monthly average groundwater levels were calculated for each observation well. Finally, the period with the most complete monthly data for each well was used for the analysis. ENSO phase effects on monthly groundwater levels were studied using groundwater anomalies, which were calculated by subtracting the historical (period of record) monthly average GW levels from the time series of monthly average GW levels. Thus, a negative anomaly indicates a lower monthly GW level than the historical, or normal, monthly average GW level, and a positive anomaly indicates a higher than normal GW level. For the wavelet analysis, the wells with the most complete data were used. Average GW levels for months having five or fewer missing daily values were calculated by ignoring the missing data and computing the monthly average GW levels.

WAVELET ANALYSIS

Hydrological time series are statistically non-stationary (Coulibaly and Baldwin, 2005). The series may exhibit periodic signals that can vary in amplitude and frequency during the historical time period. Wavelet analysis examines the relationship between two time series to determine the prevailing modes of variability and their variation over the time period. In this study, wavelet analysis was used to quantify and visualize statistically significant changes in ENSO SST anomalies and GW level variance during the historical time period. Using wavelet analysis, the magnitude and frequency of occurrence of ENSO phases and their relationship (co-variance, shared power, and phase correlations) to GW level anomalies can be detected over a

multi-decadal time scale. Wavelet analysis was done for wells under three overburden conditions: (1) well 08G001 with overburden less than 50 ft (shallow aquifer), (2) well 10G313 with overburden of 50 to 100 ft (moderately deep aquifer), and (3) well 15L020 with overburden greater than 100 ft (deep aquifer). Wavelet analysis was conducted to determine if GW levels respond to changes in ENSO SST anomalies. In the following discussion, we provide brief explanations of the wavelet analyses performed in this study. More detail can be found in Torrence and Compo (1998).

Continuous Wavelet Transform (CWT)

The CWT analyses localize recurrent oscillations in time series by transforming them into time and frequency space. Any time series x_n ($n = 0 \dots N-1$) with time spacing δt has a wavelet function $\Psi_0(\eta)$ with zero mean and is localized in time and frequency space. The choice of the wavelet function is determined by the data series. This analysis uses the Morlet wavelet function, which depends on a non-dimensional frequency ω_0 (default value 6) and non-dimensional time parameter η :

$$\Psi_0(\eta) = \pi^{-1/4} e^{-i\omega_0\eta} e^{-\eta^2/2} \quad (1)$$

The continuous wavelet transform $W_n(s)$ of a discrete sequence x_n , which is a scaled and translated version of $\Psi_0(\eta)$, is given by the following equation:

$$W_n(s) = \sum_{n'=0}^{n-1} X_{n'} \Psi^* \left[\frac{(n' - n)\delta t}{s} \right] \quad (2)$$

where n' is the translated time index, n is the localized time index, s is the wavelet scale, Ψ is the normalized wavelet, and (*) is the complex conjugate. The null hypothesis is that the signal is created by a static process with a background power spectrum (P_k), and the statistical significance of the wavelet power can be assessed relative to the null hypothesis. Time series can generally be modeled by a first-order autoregressive (AR1) method (Grinsted et al., 2004). The equation of the Fourier power spectrum of an AR1 process (Allen and Smith, 1996) is given by:

$$P_k = \frac{1 - \alpha^2}{|1 - \alpha e^{-2i\pi k}|^2} \quad (3)$$

where k is a Fourier frequency index, and α is autocorrelation at lag-1.

Cross-Wavelet Transform (XWT) and Wavelet Coherence Transform (WCT)

Although regions of high power can be seen in the WCT, a direct analysis of two time series will help in finding distinct regions of high shared power and thus significance. XWT examines whether regions in time-frequency space with high common power have a consistent phase relationship, suggestive of causality between the time series (Grinsted et al., 2004). For two time series X and Y , with different wavelet transforms $W_{nX}(s)$ and $W_{nY}(s)$, the cross-wavelet transform is defined as:

$$W_n^{xy}(s) = W_n^X(s) W_n^{Y*}(s) \quad (4)$$

where $|W_n^{xy}(s)|$ is the cross-wavelet power, and (*) represents the complex conjugate. In addition to XWT, WCT was used to evaluate the local co-variance of the two time series in time-frequency space, which may or may not exhibit high power. As XWT lose significance in visualizing shared power, WCT finds larger significant areas compared to XWT. The wavelet coherence transform for two time series (Grinsted et al., 2004) is given by:

$$R_n^2 = \frac{|S(s^{-1}W_n^{XY}(s))|^2}{S(s^{-1}|S(W_n^X(s))|^2) \cdot S(s^{-1}|S(W_n^Y(s))|^2)} \quad (5)$$

where S is a smoothing operator for the wavelet function. This expression resembles the correlation coefficient, indicating that wavelet coherence is actually correlation in time-frequency space. Statistical significance levels for the wavelet coherence were evaluated using Monte Carlo methods. XWT and WCT were performed on Niño-3.4 SST time series with GW level anomalies for different overburden conditions, calculated to 95% significance levels. The software package used for CWT, XWT, and WCT analyses was from the Matlab code developed by Aslak Grinsted (<http://noc.ac.uk/using-science/crosswavelet-wavelet-coherence>).

GROUNDWATER LEVEL FLUCTUATION AND CLIMATE VARIABILITY ANALYSIS

Monthly GW level anomalies were sorted by La Niña phases and averaged by recharge (December to April) and non-recharge (May to November) months for all the observation wells. El Niño and La Niña phases of the ENSO cycle were analyzed to study the effects of drought periods on GW level anomalies. The year 2000-2001 was especially analyzed to study the effects of strong La Niña events (prolonged droughts) on GW level anomalies. Non-parametric Mann-Whitney tests were used to evaluate the impacts of ENSO phases on the medians of GW level anomalies in the ACF. The Mann-Whitney tests assess whether the observations in one sample tend to be higher than another, make no assumption of normality, and consider the same distribution for both the samples.

RECOVERY PERIOD

For this study, groundwater recovery was associated with the criteria of six consecutive 3-month running averages (CMRA) of GW level anomalies above -0.25 ft after the end of the La Niña phase. The recovery period was calculated by the time required for the GW levels to meet the CMRA criteria after the end of the La Niña phase. Due to the lack of definitive criteria to study groundwater recovery, the CMRA criteria provided a good representation of the recovery periods. For the calculation of the recovery periods, two particular La Niña event years (1988-1989 and 2000-2001) were used, representing short and prolonged La Niña (drought) occurrences, respectively.

RESULTS

WAVELET ANALYSIS

The wavelet power spectra for Niño-3.4 SST, and GW level anomalies for wells 08G001 (shallow), 10G313 (moderately deep), and 15L020 (deep) are shown in figure 3. As previously known (Wang and Wang, 1996; Torrence and Compo, 1998), SST power is concentrated within the band group of 3 to 7 years, although the dominant modes and magnitude tend to shift with time.

Groundwater levels in the ACF basin follow the distinct pattern of seasonality of precipitation in the Southeast U.S. Groundwater levels in the ACF basin reach a yearly maximum from late winter to early spring due to steady rain, low evapotranspiration, and low agricultural pumping in winter months. Groundwater levels start declining during the growing season due to decrease in recharge by precipitation and are at yearly lows during the mid-fall (Torak and Painter, 2006). Seasonal GW level fluctuations vary throughout of the study area (Torak and Painter, 2006). Groundwater levels fluctuate more where the USCU is thin (less than 30 ft) or absent due to direct infiltration (where the USCU is absent) and vertical downward leakage (recharge) from and/or through the USCU. The wavelet power spectra used GW levels that spanned 1977 to 2012 for well 08G001 and 1976 to 2012 for wells 10G313 and 15L020. For wells 08G001 and 10G313, regions of high power relative to noise background, although not statistically significant, are seen in the wavelet power spectra in the 3 to 7 year periodicities (figs. 3b and 3c), which are similar to the periodicities in Niño-3.4 SST (fig. 3a). Both wells showed strong power in the periodicities of 3 to 5 years and 4 to 7 years during 1982 to 1990 and 1995 to 2005, respectively (figs. 3b and 3c), although the power is not statistically significant for well 08G001. High and significant power are seen in wells 08G001 and 10G313 in the 1 to 2 year period, which is perhaps related to seasonal storms

or La Niña events during 1989 to 1990 and 1999 to 2001.

High power was not seen in any periodicities for well 15L020 (fig. 3d). The high power 3 to 7 year periodicities observed in the wavelet spectra of wells 08G001 and 10G313 and the lack of such power in well 15L020 suggest that GW levels in shallow and moderately deep overburden conditions exhibit ENSO teleconnection, while such a teleconnection is missing under deep overburden conditions.

CROSS-WAVELET ANALYSIS

Unlike wavelet power spectra, where two time series show high common power independently, cross-wavelet spectra analyze the two time series directly. Significance levels for the cross-wavelet transform between Niño-3.4 SST anomalies and monthly GW level anomalies are calculated against regions of red noise background delineated with thick black outlines in figures 4a to 4c. The cross-wavelet transform between SST and GW level anomalies indicates high shared power in areas that also share high power in the single wavelet spectra. That is, wells 08G001 and 10G313 shared high and significant power in periodicities of 3 to 5 years and 4 to 7 years from 1982 to 1990 and 1995 to 2005, respectively (figs. 4a and 4b). Both wells shared high power in the 3 to 7 year periodicities, and the significant areas within these periodicities are positively phase locked. This suggests causality between SST and GW level anomalies, which attest to ENSO being the major climate variability phenomenon in the Southeast U.S.

The cross-wavelet spectra for well 15L020 did not indicate shared high and significant power in any period. It can be inferred from this lack of shared high and significant power in the cross-wavelet spectra that GW levels under deep overburden conditions are not affected by ENSO because of the high thickness of the USCU having low water-bearing properties, which restricts recharge of the UFA by vertical leakage in seasonal response to ENSO-produced

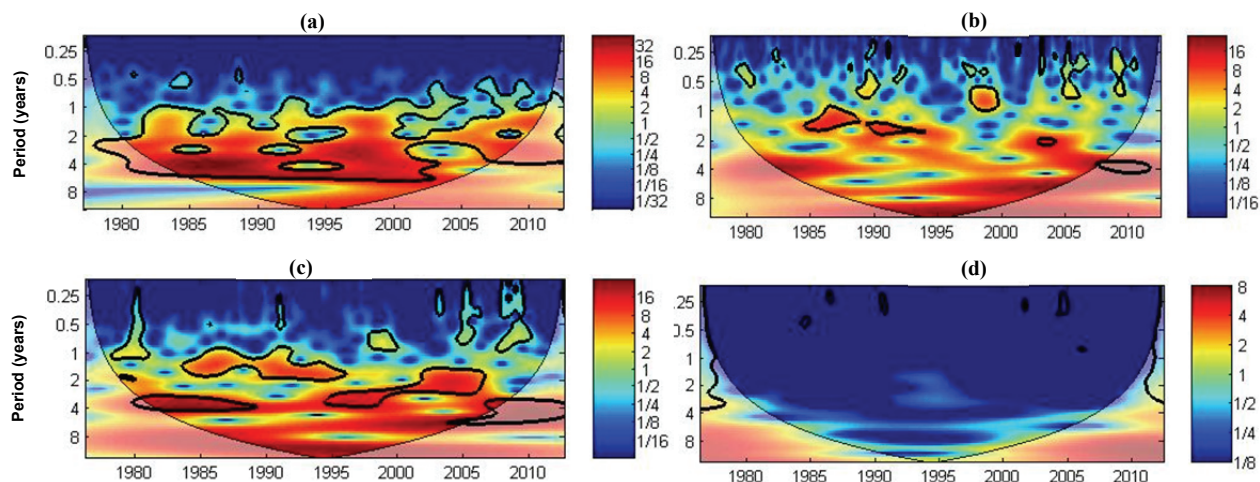


Figure 3. Significant wavelet power spectra shown within the cone-of-influence for (a) monthly Niño-3.4 sea surface temperatures ($^{\circ}\text{C}$), (b) GW level anomalies (ft) for well 08G001, (c) GW level anomalies (ft) for well 10G313, (d) GW level anomalies (ft) for well 15L020. Cool colors (blues and white) indicate low wavelet power; warm colors (reds and oranges) indicate high wavelet power. Black outlines indicate areas significant at the 95% confidence level.

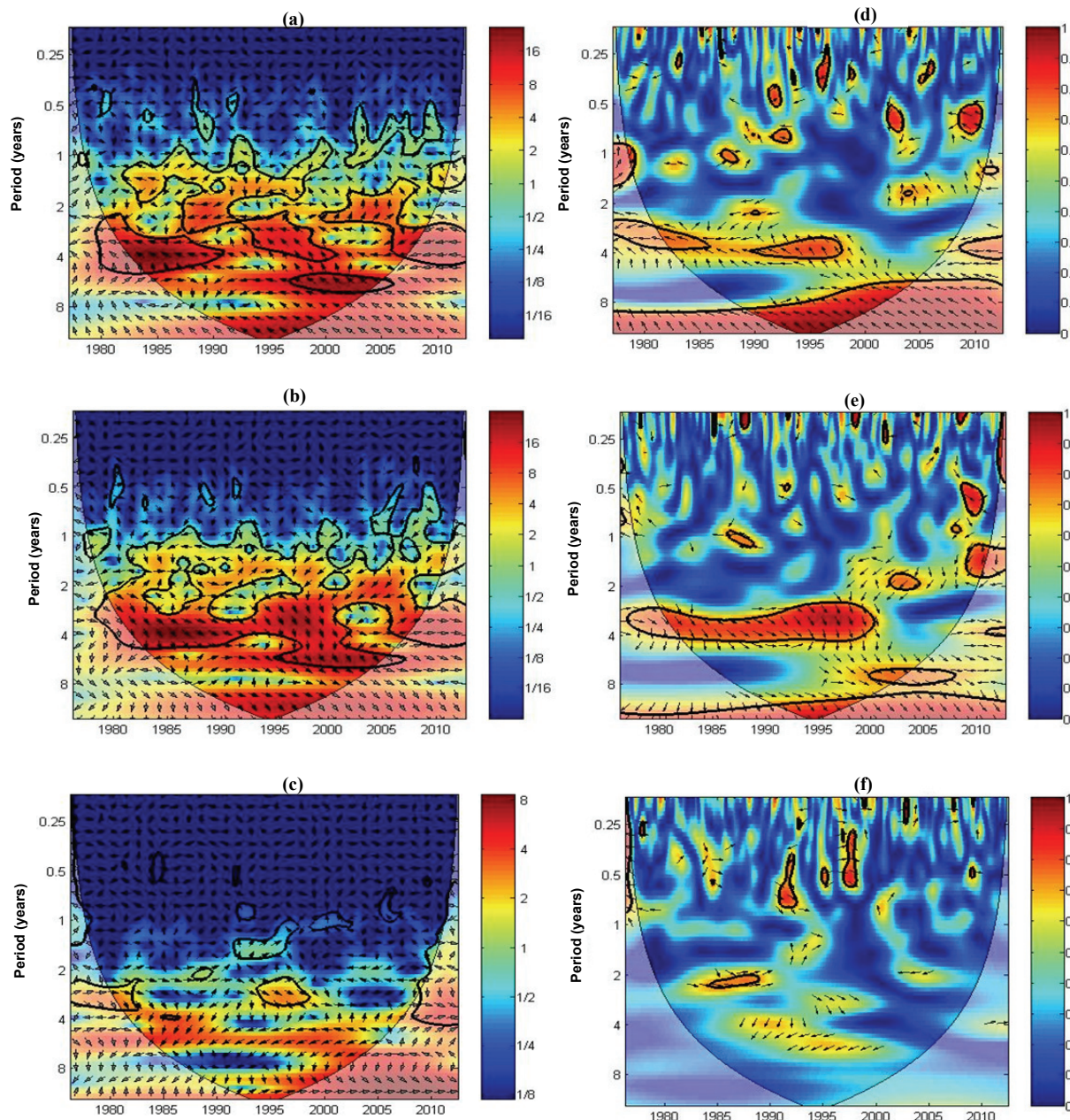


Figure 4. Cross-wavelet spectrum between Niño-3.4 sea surface temperatures and monthly GW level anomalies (ft) for wells (a) 08G001, (b) 10G313, and (c) 15L020, and wavelet coherence analysis between Niño-3.4 sea surface temperatures and monthly GW level anomalies (ft) for wells (d) 08G001, (e) 10G313, and (f) 15L020. Black outlines indicate areas significant at the 95% confidence level. Arrows indicate variable's phase relationship. Arrows pointing counter-clockwise represents anti-phase behavior, while clockwise arrows indicate in-phase behavior.

variations in precipitation.

WAVELET COHERENCE TRANSFORM

WCT for Niño-3.4 SST and GW level anomalies for wells under different overburden conditions are shown in figures 4d to 4f. Significant commonality in cross-wavelet transform spectra and wavelet coherence transform analysis does not necessarily translate to causality, as significant correlation between the two variables being investigated could occur by chance. Although small significant areas in wavelet coherence transform likely can occur by chance

and would not necessarily indicate causality, large areas of significance are unlikely due to chance and should be further examined for relationships between the two series.

WCT for Niño-3.4 SST and GW level anomalies for well 08G001 (fig. 4d) delineate small areas that have high and significant power corresponding with 3 to 7 year periodicities and are positively phase locked. These small but significant areas also shared high power in the cross-wavelet spectrum (fig. 4a) in a phase-locked condition, implying a causal relation between SST and groundwater level anomalies. More areas having high and significant

power were prevalent in the WCT for well 10G313 (fig. 4e) than for well 08G001 (fig. 4d). For well 10G313, the WCT indicates high and significant power with 3 to 4 year periodicities and phase lock during 1982 to 2000. These areas of shared power in WCT also shared power in the cross-wavelet spectra (fig. 4b), further supporting causality. WCT for well 15L020 (fig. 4f) did not indicate significant areas of high power, implying a non-causal relationship. The results of wavelet power spectra, XWT, and WCT demonstrates that groundwater levels in wells 08G001 and 10G313 exhibit ENSO teleconnection in shallow and moderately deep overburden conditions, while groundwater levels under deep overburden conditions (well 15L020) do not show any such relationship.

MANN-WHITNEY TESTS

In the previous sections, teleconnections between GW level anomalies and ENSO phases were inferred from wavelet analysis. Further analysis of 21 wells identified a high level of significant difference ($p < 0.01$) between the El Niño and La Niña phase GW level anomalies for all wells, except for well 15L020 (table 1). The median GW level anomalies during the El Niño and La Niña phases were above and below average, respectively. Ropelewski and Halpert (1986) found that El Niño and La Niña conditions were associated with above and below average precipitation, respectively, in the Southeast U.S., which explains the results in table 1 that consider the connection between precipitation and groundwater levels in the UFA. Well 08K001 showed the highest increase in the median of GW level anomalies during the El Niño phase, having a median GW level anomaly of 5.74 ft. The highest decline in GW levels during the La Niña phase is seen in well 08G001,

with a GW level anomaly of -5.50 ft (table 1). The differences in GW level anomalies for El Niño and La Niña varied for different wells, with the highest difference of approximately 9 ft occurring in well 08G001 and a low of 0.48 ft occurring in well 10K005 (table 1). The medians of monthly GW level anomalies for all wells during the El Niño and La Niña phases were 1.36 and -2.02 ft, respectively (table 1).

The El Niño and La Niña phases affected GW level anomalies differently during recharge and non-recharge seasons, resulting in larger anomalies during the recharge season than during the non-recharge season, with a few exceptions (table 2). It is important to note that ENSO phases predominantly influence winter precipitation in the Southeast U.S. (Sharda et al., 2012; Hanson and Maul, 1991a, 1991b; Schmidt et al., 2001), which explains the occurrence of larger differences in GW level anomalies during the recharge season compared to the non-recharge season. The difference in GW level anomalies between the two ENSO phases during the recharge season is approximately 2.5 times that of the non-recharge season. All wells, except 15L020, showed significant differences in GW level anomalies during the recharge season, while 17 wells showed significant differences during the non-recharge season (table 2).

Figure 5 shows the distribution of differences in GW level anomalies during recharge and non-recharge seasons corresponding with the different ENSO phases. The distribution of differences in GW level anomalies during recharge and non-recharge seasons corresponding with the two ENSO phases varies considerably by geohydrologic zone (GHZ). Figure 5 shows that during non-recharge seasons, wells in the Solution Escarpment GHZ (well 13J004) and Solution Escarpment Upland GHZ (well 15L020) did not show any significant difference. In contrast, significant differences in groundwater anomalies were exhibited during the recharge season in wells located in the Solution Escarpment GHZ but not in the Solution Escarpment Upland GHZ. Except for wells 09F520 and 11K015 during the non-recharge season, all wells in the Upland Interstream Karst and Interstream Karst GHZs showed significant difference in both the seasons. The variation in differences in GW level anomalies during the two ENSO phases throughout the GHZs indicates that overburden conditions alone do not contribute to the fluctuations in GW levels. This suggests that other factors, such as proximity to streams and lakes, and the distribution of GW withdrawal for irrigation, municipal, and industrial use, also play an important role in the development of GW level anomalies. These factors uniquely combine at every location with uncertainty in the hydraulic properties of the UFA system that govern vertical leakage, regional GW flow and storage, and GW and surface water exchange, and hence add uncertainty to the recharge in the UFA.

Table 1. Mann-Whitney test results for ENSO phases and monthly GW level anomalies during the entire period of record (p-values are significant at 0.01).

Well	El Niño ^[a] (ft)	La Niña ^[a] (ft)	Diff. ^[b] (ft)	p Value
06F001	1.35	-3.96	5.30	0.0000
09F520	0.31	-0.62	0.93	0.0000
09G001	1.01	-2.02	3.03	0.0000
10G313	0.72	-2.82	3.54	0.0000
08G001	3.66	-5.50	9.16	0.0000
11J012	0.88	-1.56	2.44	0.0000
13J004	1.32	-1.53	2.85	0.0000
08K001	5.74	-2.42	8.16	0.0000
12K014	0.98	-1.56	2.54	0.0000
13K014	1.32	-2.41	3.73	0.0000
11K003	3.35	-1.52	4.87	0.0000
13L012	0.73	-1.55	2.28	0.0000
12L030	2.33	-2.56	4.88	0.0000
12L028	1.76	-3.19	4.96	0.0000
13L049	2.89	-3.68	6.57	0.0000
12M017	2.20	-1.38	3.58	0.0000
13M006	3.24	-1.62	4.86	0.0000
07H002	3.79	-2.76	6.56	0.0000
12L029	1.82	-2.24	4.07	0.0000
11K015	0.36	-2.03	2.39	0.0000
10K005	0.29	-0.19	0.48	0.0000
15L020 ^[c]	0.60	-1.95	2.56	0.4129
Median	1.36	-2.02	3.66	

^[a] Values indicate the median for each well.

^[b] Difference in median for El Niño and La Niña phase.

^[c] Non-significant well.

Table 2. Mann-Whitney test results of differences in median monthly GW level anomalies caused by El Niño and La Niña phases during recharge and non-recharge seasons (p-values are significant at 0.05).

Well	Recharge Season				Well	Non-Recharge Season			
	El Niño ^[a] (ft)	La Niña ^[b] (ft)	Diff. ^[c] (ft)	p Value		El Niño ^[a] (ft)	La Niña ^[b] (ft)	Diff. ^[c] (ft)	p Value
06F001	5.40	-5.77	11.17	0.0000	06F001	0.10	-3.38	3.48	0.0001
09F520	1.44	-0.83	2.27	0.0000	09F520 ^[d]	-0.23	-0.29	0.06	0.3801
09G001	3.01	-2.72	5.73	0.0000	09G001	0.59	-1.66	2.25	0.0000
10G313	1.91	-3.37	5.29	0.0000	10G313	-0.30	-2.40	2.10	0.0026
08G001	7.31	-7.93	15.23	0.0000	08G001	2.18	-4.35	6.53	0.0000
11J012	2.08	-2.41	4.49	0.0000	11J012	0.56	-0.89	1.45	0.0000
13J004	2.22	-3.37	5.59	0.0000	13J004 ^[d]	0.31	-0.75	1.05	0.1152
08K001	4.54	-2.21	6.75	0.0000	08K001	6.27	-3.30	9.56	0.0000
12K014	2.56	-2.79	5.35	0.0000	12K014	0.41	-1.08	1.48	0.0001
13K014	3.12	-3.40	6.52	0.0000	13K014	0.69	-1.69	2.39	0.0000
11K003	4.61	-3.23	7.84	0.0000	11K003	2.06	-0.86	2.92	0.0376
13L012	2.19	-2.38	4.57	0.0000	13L012	0.57	-0.94	1.51	0.0010
12L030	3.64	-2.77	6.42	0.0000	12L030	1.47	-2.45	3.92	0.0019
12L028	4.02	-4.06	8.08	0.0000	12L028	0.51	-3.17	3.68	0.0136
13L049	6.31	-4.42	10.73	0.0000	13L049	1.17	-2.82	3.99	0.0006
12M017	2.94	-1.96	4.90	0.0000	12M017	1.06	-0.71	1.77	0.0285
13M006	3.35	-1.51	4.86	0.0000	13M006	2.93	-1.73	4.66	0.0000
07H002	3.78	-2.47	6.25	0.0000	07H002	3.81	-4.16	7.97	0.0000
12L029	3.14	-2.87	6.01	0.0000	12L029	1.02	-1.78	2.81	0.0040
11K015	3.34	-3.21	6.54	0.0000	11K015 ^[d]	-0.41	-1.26	0.86	0.9206
10K005	0.33	-0.39	0.73	0.0000	10K005	0.26	0.08	0.19	0.0311
15L020 ^[d]	0.7	-3.91	4.61	0.1559	15L020 ^[d]	0.53	1.28	-0.75	0.7482
Median	3.13	-2.83	6.13		Median	0.58	-1.68	2.32	

^[a] Values indicate the median monthly groundwater level anomalies for each well for the El Niño phase.

^[b] Values indicate the median monthly groundwater level anomalies for each well for the La Niña phase.

^[c] Difference in median monthly groundwater level anomalies for El Niño and La Niña phases.

^[d] Non-significant wells.

Table 3 shows the mean GW level anomalies during an average La Niña phase and for 2000-2001 (representing a severe La Niña event). Comparison of mean GW level anomalies resulting from average and severe La Niña events indicates that severe La Niña events, such as the one that occurred during 2000-2001, yield, on average, twice the negative anomalies as those resulting from an average La Niña phase (table 3). Unlike an average La Niña phase (where GW level anomalies differ during the recharge and non-recharge seasons), GW level anomalies associated with

the severe La Niña event of 2000-2001 exhibited similarities in magnitude during the recharge and non-recharge seasons. Groundwater levels in nearly all wells yielded larger negative anomalies during the severe La Niña event than during the average La Niña phase. Maximum negative GW level anomalies for 2000-2001 were nearly 3.25 to 5.12 times larger than anomalies associated with average La Niña phases during recharge and non-recharge seasons. Negative GW level anomalies exceeded -10 ft at eight wells and -5 ft at 20 wells. In wells 08G001, 08K001, and

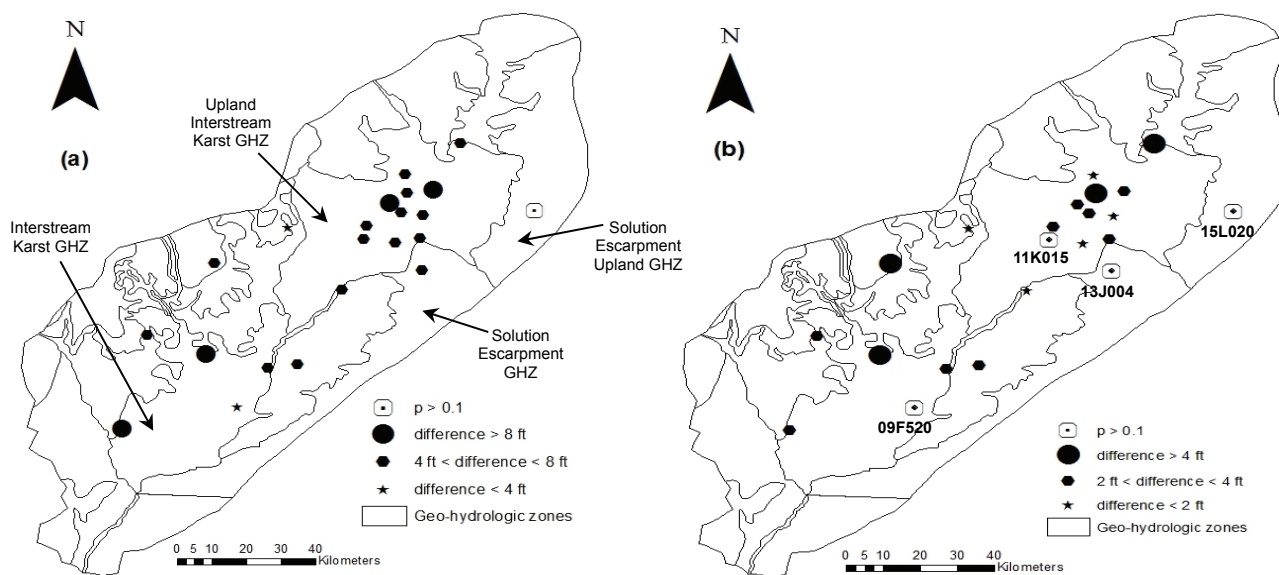


Figure 5. Distribution of differences in groundwater level anomalies produced by El Niño and La Niña phases during (a) recharge and (b) non-recharge seasons (GHZ = geo-hydrologic zone).

Table 3. Comparison of monthly average GW level anomalies for severe (2000-2001) and average La Niña phases during recharge and non-recharge seasons.

Well	Recharge		Non-Recharge		2000-2001 Minimum
	Average	Severe	Average	Severe	
06F001	-5.20	-4.49	-2.86	-4.24	-10.44
09F520	-1.11	-3.23	-0.19	-3.16	-5.13
09G001	-2.00	-3.34	-1.35	-3.00	-5.22
10G313	-2.90	-6.70	-2.15	-6.38	-9.60
08G001	-5.83	-8.83	-3.68	-7.90	-14.31
11J012	-1.93	-2.52	-0.98	-2.07	-4.64
13J004	-2.54	-5.91	-0.94	-5.92	-8.13
08K001	-3.58	-3.02	-3.48	-6.19	-15.26
12K014	-2.49	-3.32	-1.13	-2.62	-6.01
13K014	-2.76	-3.64	-1.57	-3.03	-6.31
11K003	-3.21	-8.47	-1.26	-7.37	-13.66
13L012	-1.88	-2.57	-0.84	-2.70	-5.11
12L030	-2.28	-3.79	-1.65	-3.83	-6.71
12L028	-3.56	-6.21	-2.09	-4.73	-10.13
13L049	-3.57	-6.13	-2.12	-5.38	-8.50
12M017	-1.69	-2.21	-1.13	-1.39	-8.84
13M006	-1.93	-2.06	-3.01	-3.93	-17.43
07H002	-2.56	-3.19 ^[a]	-1.77	-2.18 ^[a]	-5.83
12L029	-3.79	-3.70	-3.76	-4.96	-10.44
11K015	-3.78	-9.07	-1.03	-7.15	-14.38
10K005	-0.51	-0.32 ^[a]	-0.49	-1.93 ^[a]	-5.48
Mean	-2.81	-4.42	-1.78	-4.29	-9.12

^[a] For year 2000 only.

13M006, negative groundwater level anomalies exceeded -15 ft during 2000-2001, which demonstrates the effect of a severe and prolonged La Niña phase on groundwater levels (table 3). GW level depletion during prolonged droughts is caused not only by decreased precipitation but also by increased agricultural pumping. The results in table 3 demonstrate the combined effect of these two aspects on GW levels in the area. Such a drastic fall in GW levels can lower streamflows in the Flint River and prohibit meeting the minimum flow requirements in the Flint and Apalachicola Rivers.

RECOVERY PERIOD

Recovery in GW levels following La Niña events varies according to the severity of the phase. On average, the severe La Niña phase during 2000-2001 required a significantly longer recovery time (22 months) than the short La Niña event during 1988-1989 (2 months) (table 4). During 2000-2001, GW levels tended to recover during the end of the La Niña phase (March 2001), although not always exhibiting positive anomalies. However, with the onset of the growing season in April 2001, GW levels declined to further low levels as a result of increased irrigation and evapotranspiration demands. The recovery period for wells during 2000-2001 varied from 18 to 26 months, except for wells 12M017 and 07H002, which recovered within a month, thus meeting the six consecutive 3-month running average (CMRA) criteria. However, GW levels in these two wells also fell below normal with the onset of pumping during the growing season.

The recovery time for wells during the short-duration La Niña phase of 1988-1989 varied from 0 to 9 months (table 4). Recovery time for wells 10G313, 13J004, 12L028, and 11K015 exceeded 5 months, even though all other wells exhibited a recovery period of 2 months or less. This again can be explained by the unique hydraulic characteris-

Table 4. Comparison of recovery periods (months) for prolonged (2001) and short (1989) La Niña phases.

Well	2001	1989
06F001	18	1
09F520	23	2
09G001	25	2
10G313	24	8 ^[a]
08G001	18	1
11J012	24 ^[c]	1
13J004	28 ^[a]	9 ^[a]
08K001	18 ^[c]	0
12K014	24 ^[c]	1
13K014	24 ^[c]	1
11K003	25	2
13L012	25	0
12L030	26	2
12L028	26	6
13L049	26	1
12M017	1 ^[b]	1
13M006	25	1
07H002	0 ^[b]	2 ^[a]
12L029	25	1
11K015	25	8 ^[a]
10K005	25	0
Mean	22	2

^[a] Did not meet the six consecutive 3-month running average criteria.

^[b] Met the six consecutive 3-month running average criteria followed by negative anomalies due to onset of growing season (April 2001).

^[c] Showed positive anomalies for a brief period at the end of the La Niña phase (March 2001) but did not meet the six consecutive 3-month running average criteria.

tics at each well location, which is responsible for the inconsistent GW level fluctuations and recovery throughout the study area. Tables 3 and 4 show that GW resources are vulnerable during severe La Niña events, and dependence on GW needs to be reduced immediately when a severe La Niña is forecasted. Considering the UFA-FR connectivity, reducing dependence on GW for irrigation during severe La Niña events may help ensure minimum levels of streamflow in the river.

SUMMARY AND CONCLUSION

This study used wavelet analysis and the non-parametric Mann-Whitney test to identify and quantify the teleconnection between the climate variability phenomenon known as the El Niño Southeast Oscillation (ENSO) and groundwater (GW) levels in the lower Apalachicola-Chattahoochee-Flint river basin. Wavelet analysis was used to find teleconnection between Niño-3.4 sea surface temperature anomalies and GW level anomalies, while the Mann-Whitney test was used to quantify this teleconnection. Analysis of GW level fluctuations in the event of a severe drought (prolonged La Niña phase) was also performed to estimate recovery periods.

Results of wavelet analysis indicated that wells representing shallow and moderately deep overburden conditions respond to ENSO in periodicities of 3 to 7 years. The well in deep overburden did not respond to short-term climate fluctuations, indicating that GW levels under deep overburden conditions are not affected by ENSO. Mann-Whitney tests found significant differences ($p < 0.01$) in GW level anomalies between the two ENSO phases (El Niño and La Niña) for all wells except the well in deep overburden. GW levels were higher than the long-term av-

erage during El Niño phases while lower than average during La Niña phases. The results of the Mann-Whitney tests confirmed the results of the wavelet analysis. Analysis for recharge and non-recharge periods indicated that ENSO-induced anomalies were approximately 2.5 times greater during the recharge season than during for the non-recharge season, which is in agreement with previous studies that indicate the predominant effect of ENSO on winter precipitation and temperature in the Southeast U.S.

Comparison of La Niña phases representing severe (2000-2001) and average conditions indicated that average GW levels dropped approximately twice as much during the severe La Niña as compared to the average La Niña during recharge and non-recharge seasons. Unlike the average La Niña phase, where GW level anomalies are large during the recharge season, the severe La Niña event during 2000-2001 produced similar GW level anomalies for both the recharge and non-recharge seasons, which could be due to increased irrigation during the non-recharge season stemming from prolonged drought conditions. Recovery times for the severe La Niña during 2000-2001 were significantly longer (22 months vs. 2 months) than those during the short La Niña of 1988-1989.

The results of this study illustrate that La Niña severely impacts GW levels in the study area, especially during severe events. The prolonged recovery periods during severe droughts validate the point that GW level fluctuates at a different time scale as compared to soil moisture and streamflows. Therefore, this study suggests that GW levels should also be used (in combination with precipitation deficit, soil moisture, streamflows, and other factors) as an indicator of drought in this area. It was also found that the role of irrigation cannot be ignored for such large recovery periods because GW level depletions during droughts are caused not only by the lack of precipitation but also by increased irrigation pumping. It was also found that GW levels are affected by local geohydrologic characteristics. Therefore, in order to use GW levels as an indicator of drought in this region, a number of wells in different geologic formations and overburden conditions should be used. Further, although ENSO forecasts (e.g., those issued by the NOAA Climate Prediction Center and the International Research Institute at Columbia University) can be used to forecast GW levels, reduce irrigation pumping based on those forecasts, and maintain streamflows in the Flint and Apalachicola Rivers, ENSO forecasts should be combined with a detailed GW model and irrigation water withdrawal projections to develop an effective GW level forecasting methodology. Such a modeling effort will also help identify critical areas where timely reductions in irrigation water withdrawal will help maintain streamflows. This would help resolve the complex water management issues and conflicts (i.e., the tri-state water wars) in this region.

ACKNOWLEDGEMENTS

The authors wish to acknowledge funding provided for this study by the NOAA Sectoral Applications Research Program (SARP), the National Integrated Drought Information System (NIDIS), and the NOAA Regional Integrated Sciences and Assessments (RISA) Program. We also

wish to acknowledge Lynn Torak from the USGS Georgia Water Science Center for his invaluable input on this paper.

REFERENCES

- Aceituno, P. (1992). El Niño, the southern oscillation, and ENSO: Confusing names for a complex ocean-atmosphere interaction. *Bull. American Meteorol. Soc.*, 73(4), 483-485.
- Allen, M. R., & Smith, L. A. (1996). Monte Carlo SSA: Detecting irregular oscillations in the presence of colored noise. *J. Climate*, 9(12), 3373-3404. [http://dx.doi.org/10.1175/1520-0442\(1996\)009<3373:MCSPIO>2.0.CO;2](http://dx.doi.org/10.1175/1520-0442(1996)009<3373:MCSPIO>2.0.CO;2).
- Chiew, F. H. S., Piechota, T. C., Dracup, J. A., & McMahon, T. A. (1998). El Niño/Southern Oscillation and Australian rainfall, streamflow, and drought: Links and potential for forecasting. *J. Hydrol.*, 204(1-4), 138-149. [http://dx.doi.org/10.1016/S0022-1694\(97\)00121-2](http://dx.doi.org/10.1016/S0022-1694(97)00121-2).
- Coulibaly, P., & Baldwin, C. K. (2005). Nonstationary hydrological time series forecasting using nonlinear dynamic methods. *J. Hydrol.*, 307(1-4), 164-174. <http://dx.doi.org/10.1016/j.jhydrol.2004.10.008>.
- Diaz, H. F., & Markgraf, V. (1992). *El Niño: Historical and Paleoclimatic Aspects of the Southern Oscillation*. Cambridge, U.K.: Cambridge University Press.
- Enfield, D. B., Mestas-Nuez, A. M., & Trimble, P. J. (2001). The Atlantic multi-decadal oscillation and its relation to rainfall and river flows in the continental U.S. *Geophysical Res. Letters*, 28(10), 2077-2080. <http://dx.doi.org/10.1029/2000GL012745>.
- Grinsted, A., Moore, J., & Jevrejeva, S. (2004). Application of the cross-wavelet transform and wavelet coherence to geophysical time series. *Nonlinear Proc. Geophysics*, 11(5-6), 561-566. <http://dx.doi.org/10.5194/npg-11-561-2004>.
- Gurdak, J. J., Hanson, R. T., McMahon, P. B., Bruce, B. W., McCray, J. E., Thyne, G. D., & Reedy, R. C. (2007). Climate variability controls on unsaturated water and chemical movement, High Plains aquifer, USA. *Vadose Zone J.*, 6(3), 533-547. <http://dx.doi.org/10.2136/vzj2006.0087>.
- Hansen, D. V., & Maul, G. A. (1991a). Anticyclonic current rings in the eastern tropical Pacific Ocean. *J. Geophysical Res.*, 94(C4), 6965-6979. <http://dx.doi.org/10.1029/91JC00096>.
- Hanson, K., & Maul, G. A. (1991b). Florida precipitation and the Pacific El Niño, 1895-1989. *Florida Scientist*, 54(3-4), 160-168.
- Hansen, J., Jones, J., Irmak, A., & Royce, F. (2001). El Niño-Southern Oscillation impacts on crop production in the southeast United States. In *Impacts of El Niño and Climate Variability on Agriculture*, pp. 55-76. ASA Special Publication 63. Madison, Wisc.: ASA.
- IPCC. (2001). *Climate Change 2001: Impacts, Adaptations, and Vulnerability*. Contribution of working group II to the third assessment report of the Intergovernmental Panel on Climate Change. Cambridge, U.K.: Cambridge University Press.
- Johnson, N. T., Martinez, C. J., Kiker, G. A., & Leitman, S. (2013). Pacific and Atlantic sea surface temperature influences on streamflow in the Apalachicola-Chattahoochee-Flint river basin. *J. Hydrol.*, 489, 160-179. <http://dx.doi.org/10.1016/j.jhydrol.2013.03.005>.
- Jones, L. E., & Torak, L. J. (2006). Simulated effects of seasonal groundwater pumpage for irrigation on hydrologic conditions in the lower Apalachicola-Chattahoochee-Flint river basin, southwestern Georgia and parts of Alabama and Florida, 1999-2002. USGS Scientific Investigations Report 2006-5234. Reston, Va.: U.S. Geological Survey. Retrieved from <http://pubs.usgs.gov/sir/2006/5234/>.
- Kahya, E., & Dracup, J. A. (1993). U.S. streamflow patterns in relation to the El Niño/Southern Oscillation. *Water Resour.*

- Res.*, 29(8), 2491-2503. <http://dx.doi.org/10.1029/93WR00744>.
- Keener, V. W., Ingram, K. T., Jacobson, B., & Jones, J. W. (2007). Effects of El-Niño/Southern Oscillation on simulated phosphorus loading. *Trans. ASABE*, 50(6), 2081-2089. <http://dx.doi.org/10.13031/2013.24110>.
- Keener, V. W., Feyerisen, G. W., Lall, U., Jones, J. W., Bosch, D. D., & Lowrance, R. (2010). El-Niño/Southern Oscillation (ENSO) influences on monthly NO₃ load and concentration, streamflow, and precipitation in Little River watershed, Tifton, Georgia. *J. Hydrol.*, 381(3-4), 352-363. <http://dx.doi.org/10.1016/j.jhydrol.2009.12.008>.
- Kiladis, G. N., & Diaz, H. F. (1989). Global climate anomalies associated with extremes in the Southern Oscillation. *J. Climate*, 2(9), 1069-1090. [http://dx.doi.org/10.1175/1520-0442\(1989\)002<1069:GCAAWE>2.0.CO;2](http://dx.doi.org/10.1175/1520-0442(1989)002<1069:GCAAWE>2.0.CO;2).
- Kulkarni, J. R. (2000). Wavelet analysis of the association between the Southern Oscillation and the Indian summer monsoon. *Intl. J. Climatol.*, 20(1), 89-104. [http://dx.doi.org/10.1002/\(SICI\)1097-0088\(200001\)20:1<89::AID-JOC458>3.0.CO;2-W](http://dx.doi.org/10.1002/(SICI)1097-0088(200001)20:1<89::AID-JOC458>3.0.CO;2-W).
- McCabe, G. J., & Dettinger, M. D. (1999). Decadal variations in the strength of ENSO teleconnections with precipitation in the western United States. *Intl. J. Climatol.*, 19(13), 1399-1410. [http://dx.doi.org/10.1002/\(SICI\)1097-0088\(19991115\)19:13<1399::AID-JOC457>3.0.CO;2-A](http://dx.doi.org/10.1002/(SICI)1097-0088(19991115)19:13<1399::AID-JOC457>3.0.CO;2-A).
- NOAA. (2010). Cold and warm episodes by season. Camp Springs, Md.: National Oceanic and Atmospheric Administration, Climate Prediction Center. Retrieved from www.cpc.ncep.noaa.gov/products/analysis_monitoring/ensostuff/ensoyears.shtml.
- NRC. (1995). *Natural Climate Variability on Decade-to-Century Time Scales*. Washington, D.C.: National Research Council.
- Quinn, W. H. (1974). Monitoring and predicting El Niño invasions. *J. Appl. Meteorol.*, 13(7), 825-830. [http://dx.doi.org/10.1175/1520-0450\(1974\)013<0825:MAPENI>2.0.CO;2](http://dx.doi.org/10.1175/1520-0450(1974)013<0825:MAPENI>2.0.CO;2).
- Rajagopalan, B., & Lall, U. (1998). Interannual variability in western U.S. precipitation. *J. Hydrol.*, 210(1-4), 51-67. [http://dx.doi.org/10.1016/S0022-1694\(98\)00184-X](http://dx.doi.org/10.1016/S0022-1694(98)00184-X).
- Ropelewski, C. F., & Halpert, M. S. (1986). North American precipitation and temperature patterns associated with the El Niño/Southern Oscillation (ENSO). *Monthly Weather Rev.*, 114(12), 2352-2362. [http://dx.doi.org/10.1175/1520-0493\(1986\)114<2352:NAPATP>2.0.CO;2](http://dx.doi.org/10.1175/1520-0493(1986)114<2352:NAPATP>2.0.CO;2).
- Roy, S. S. (2006). The impacts of ENSO, PDO, and local SSTs on winter precipitation in India. *Physical Geography*, 27(5), 464-474. <http://dx.doi.org/10.2747/0272-3646.27.5.464>.
- Schmidt, N., & Luther, M. E. (2002). ENSO impacts on salinity in Tampa Bay, Florida. *Estuaries and Coasts*, 25(5), 976-984. <http://dx.doi.org/10.1007/BF02691345>.
- Schmidt, N., Lipp, E. K., Rose, J. B., & Luther, M. (2001). ENSO influences on seasonal rainfall and river discharge in Florida. *J. Climate*, 14(4), 615-628. [http://dx.doi.org/10.1175/1520-0442\(2001\)014<0615:EIOSRA>2.0.CO;2](http://dx.doi.org/10.1175/1520-0442(2001)014<0615:EIOSRA>2.0.CO;2).
- Sharda, V., Srivastava, P., Ingram, K., Chelliah, M., & Kalin, L. (2012). Quantification of El Niño Southern Oscillation (ENSO) impact on precipitation and streamflows for improved management of water resources in Alabama. *J. Soil Water Cons.*, 67(3), 158-172. <http://dx.doi.org/10.2489/jswc.67.3.158>.
- SELC. (2014). Tri-state water wars (AL, GA, FL). Charlottesville, Va.: Southern Environmental Law Center. Retrieved from www.southernenvironment.org/cases/tri_state_water_wars_al_ga_fl.
- Tootle, G. A., Piechota, T. C., & Singh, A. (2005). Coupled oceanic-atmospheric variability and U.S. streamflow. *Water Resour. Res.*, 41(12), W12408. <http://dx.doi.org/10.1029/2005WR004381>.
- Torak, L. J., & Painter, J. A. (2006). Geohydrology of the lower Apalachicola-Chattahoochee-Flint river basin, southwestern Georgia, northwestern Florida, and southeastern Alabama. USGS Scientific Investigations Report 2006-5070. Reston, Va.: U.S. Geological Survey.
- Torrence, C., & Compo, G. P. (1998). A practical guide to wavelet analysis. *Bull. American Meteorol. Soc.*, 79(1), 61-78. [http://dx.doi.org/10.1175/1520-0477\(1998\)079<0061:APGTWA>2.0.CO;2](http://dx.doi.org/10.1175/1520-0477(1998)079<0061:APGTWA>2.0.CO;2).
- Wang, Y., & Wang, B. (1996). Temporal structure of the Southern Oscillation as revealed by waveform and wavelet analysis. *J. Climate*, 9(7), 1586-1598. [http://dx.doi.org/10.1175/1520-0442\(1996\)009<1586:TSOTSO>2.0.CO;2](http://dx.doi.org/10.1175/1520-0442(1996)009<1586:TSOTSO>2.0.CO;2).